SOLID STATE PHYSICS

NITROGEN ADSORPTION ON GRAPHENE SPONGES SYNTHESIZED BY ANNEALING A MIXTURE OF NICKEL AND CARBON POWDERS

V. Grehov[1], J. Kalnacs[1], A. Mishnev[2], K. Kundzins[3]

[1]Institute of Physical Energetics,
11 Krīvu Str., Riga, LV-1006, LATVIA

[2]Latvian Institute of Organic Synthesis,
21 Aizkraukles Str., Riga, LV-1006, LATVIA

[3]Institute of Solid State Physics, University of Latvia,
8 Kengaraga Str., Riga, LV-1063, LATVIA

Adsorption by graphene sponge (GS) manufactured by annealing nickel-carbon powder mixture in inert atmosphere has been studied. By determining the specific surface area (SSA) for the GS sample, it has been found that Brunauer, Emmett, Teller method (BET) of approximation of experimental isotherms gives wrong results in the pressure range of 0.025–0.12 because adsorption in this pressure region is affected by walls of ampoule. Real SSA value has been found by subtracting pore effect method (SPE) or by BET approximation in a low range of relative pressure of 0.0004–0.002.

Keywords: *graphene sponge, nitrogen adsorption, specific surface area, BET approximation.*

1. INTRODUCTION

The study is dedicated to the adsorption properties of new graphenic material graphene sponge (GS) developed by the authors [1] by annealing nickel-carbon powder mixture in inert atmosphere.

Many studies have been devoted to the adsorption properties of carbon materials [2], [3]. It can be explained by a variety of morphological properties of carbon materials known as activated carbons, carbon blacks and carbon nanotubes, cones, fibres, bulbs, graphenes, graphene aerogels, foams and sponges [4], [5].

Graphene, 2D carbon allotrope, has drawn significant interest among scientists due to intriguing properties since 2004 [6]. In recent years, the assembly of graphene into macroscopic (3D) structures has attracted intensive interest because the use of 3D graphene is one of the most effective ways of applying the unique properties of 2D graphene nanosheets in practice [4], [7]. Graphene 3D structures consist of flexible graphene nanosheets, which are interconnected into porous networks.

Several different names have been used for such structures, namely, graphene foam, sponge, aerogel and monolith. Among the attractive applications, graphene sponges have been used as adsorbents for various pollutants [5]. For instance, less than 3.5 kg graphenic carbon foam can absorb 1 ton petroleum, promising great potential in the applications of oil spill and pollution treatments [7].

It is well known that the pore size and its distribution are important factors determining the adsorption properties of different adsorbents. It is of interest to relate the adsorption properties of the GS to its morphological structure and to elucidate the possibilities of changing this structure during the preparation of the GS.

2. EXPERIMENTAL

To reveal the nature of GS adsorption capacity, its specific surface and pore size distribution (PSD), the authors of the research studied the adsorption of nitrogen at 77K using Autosorb-1 device (*Quantachrome Instruments Co.*, Florida, USA). The methods of measurements were standard (see the previous article about adsorption properties of thermochemically exfoliated graphite (TEG) [8]). The level of liquid nitrogen was supported automatically. During measurement, the substance was placed into a quartz ampoule 9 mm in diameter. To reduce the empty volume, a glass rod was used.

The samples for adsorption measurements were small pieces of GS manufactured by the authors of the research [1].

The substance weight was 1–5 mg in each case. Before measuring adsorption, the GS was heated in vacuum at 300 °C for not less than 24 h, before the leak rate became lower than 10–15 micron/min. To process and present the results, ASWin v1.55 and home-made software were used.

All investigated GS samples were analysed by means of SEM (Hitachi M3000), high resolution SEM LYRA3 XMU (Tescan, Czech Republic), transmission electron microscope (TEM) Tecnai G20 (FEI) and XRD (Japan Rigaku UL-TIMA IV, Cu–Ka radiation λ = 0.154184 nm).
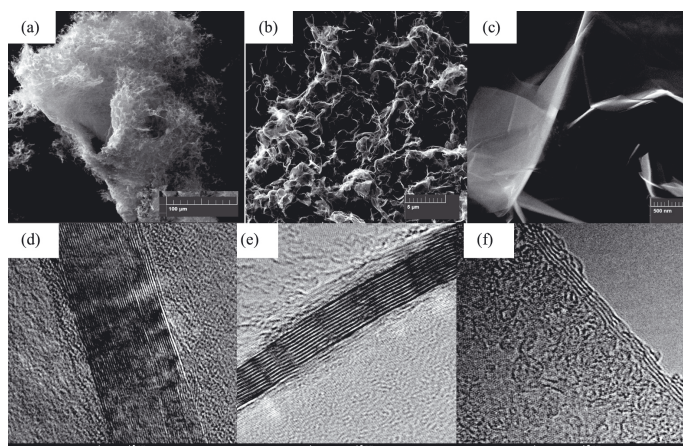

Fig. 1. High resolution SEM images (a), (b), (c) – typical GS samples, (d), (e), (f) – high resolution TEM image of the same samples after dispersion in the isopropanol by ultrasound.

3. RESULTS AND DISCUSSION

Figure 1 demonstrates typical GS images with different magnifications. It can be clearly seen that the GS consists of graphene sheets that are well-developed in the base plane (002), entangled and partly interconnected, with folds and wrinkles. The thickness of these sheets was determined from the XRD spectra by the width of the (002) peak [1]. The values obtained for the GS sheet thickness were in the range of 6–16 nm. The individual graphene sheets of GS were examined using TEM [9]. The GS material was placed in isopropanol and dispersed by ultrasound and then a drop of isoprapanol with suspended graphene sheets was applied to the grid for electronic microscopy. For TEM, a copper grid with a holey carbon film (Agar Scientific, UK) was used.

In all the GS samples studied, sheets with a different number of layers from 2 to 40 were found in approximate correspondence with the thickness obtained from the XRD data. A similar range of values of the graphene layers was shown on the multilayer graphene obtained on transition-metal foams by the chemical vapour deposition (CVD) method [10]. The dissolution of carbon in the metal takes place using CVD process [10] and Ni – carbon powder annealing methods [1]. When a carbon atom precipitates on the metal, at the cooling stage, the formation of multilayer graphene sheets occurs. The authors of the research attempted to control the number of layers in multilayer sheets of graphene by controlling carbon weight in the Ni – carbon mix [1].
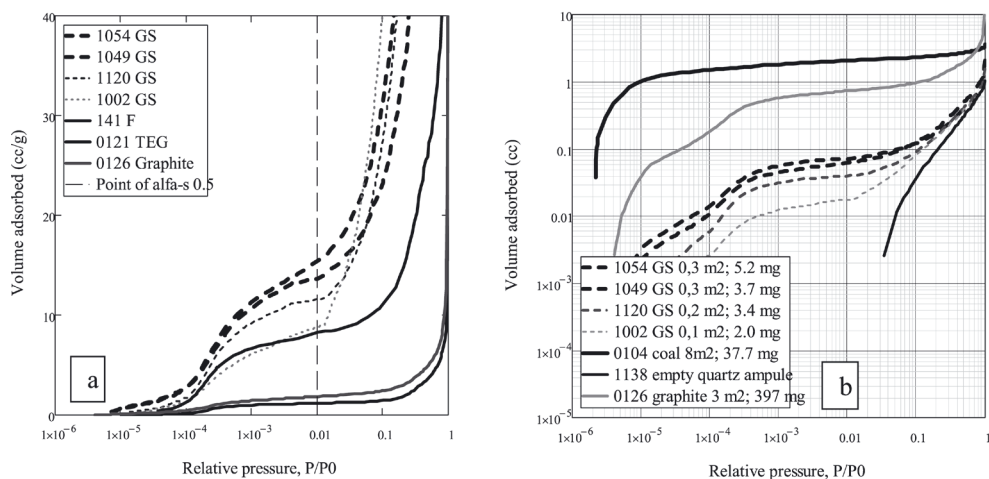

Fig. 2. N2 adsorption by grafitized carbon: graphene sponges (1054, 1049, 1120, 1002), graphitized carbon black Carbopack F (141), milled graphite (0126). a – specific volume of adsorption for different samples, b – adsorbed volume for these adsorption processes, on the inset the areas and weights of the samples are indicated.

On the multilayer graphene sheets (Fig. 1e, f), a non-uniform surface of graphene sheets can be observed; these inhomogeneities could possibly serve as the basis for the formation of micropores (<2 nm). Investigation of adsorption for the GS samples showed that it was well-graphitized carbon material.

Objects of this type are well studied on powder samples of graphitized carbon blacks [11], [12]. They are characterised by II or IV type isotherms (IUPAC [13]) depending on the absence or presence of micro and mesopores.

The authors of the research examined the isotherms of GS samples in comparison with the isotherms of other graphitized carbon samples performed by the authors earlier [8], and also during the present research (Fig. 2a). According to the characteristic form of adsorption isotherms at low pressures (smaller as ~ 0.01 P/P_0), it was clear that they referred to adsorption on a graphite surface. Further increase in adsorption observed for the GS samples at $P/P_0 \sim 0.01$–0.15 should not occur because the adsorption of the second monolayer N2 onto the graphene surface began only at $P/P_0 > 0.15$ [14]. This increase in adsorption could formally be associated with an increase in the capillary condensation in the presence of pores ~ 2 nm [15]. However, the authors of the research prefer another explanation.

The upward deviation of adsorption can be explained as follows: at pressures greater than 0.01 P/P_0, the adsorbed volume on the GS becomes smaller than the volume adsorbed on the ampoule walls, which is explained by the fact that the total amount of adsorbed volume ceases to depend on the mass of the GS and adsorption lines for different GS samples become approximately equal to the empty ampoule adsorption (Fig. 2b).
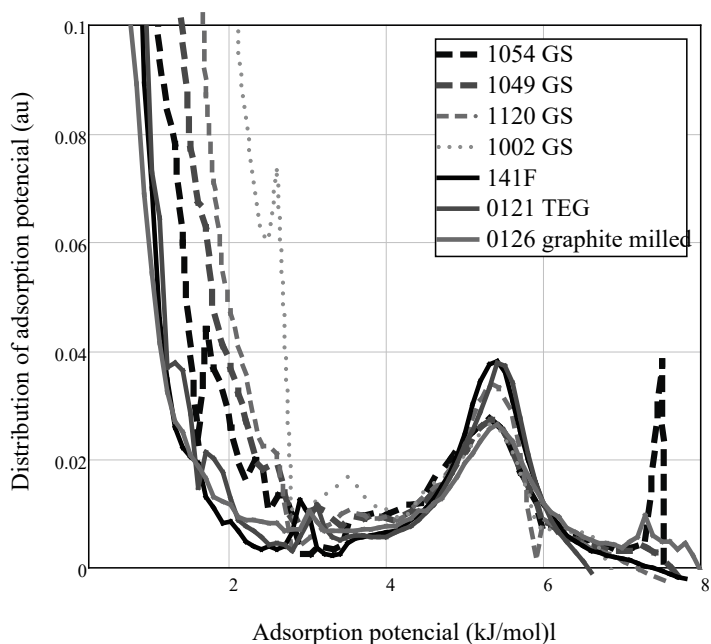

Fig. 3. Adsorption potential distribution for N2 adsorption by grafitized carbon: milled graphite, graphene sponges (GS), thermoexpholiated graphite plates (TEG) [11], graphitized carbon black Carbopack F.

It should be taken into account that in the instructions of the device manufacturer (Autosorb-1) it is explicitly stated that the area of the measured adsorbent should be 10–15 m². The area and weight of the measured samples are shown in Fig. 2b. The reason for working with such small samples of GS is related to the equipment on which the samples were obtained [1].

In further research, we believed that the growth of adsorption at pressure above ~ 0.01 P/P_0 was associated with adsorption on the ampoule walls. Fortunately, adsorption at low pressures was associated only with GS, which allowed obtaining positive results.

The distribution of the adsorption potential (APD) for all the samples studied in the research was calculated from isotherms (see Fig. 3). The adsorption potential is the energy that is released upon adsorption of N2 molecules on the adsorbing surface. On a homogeneous surface, all places have the same energy, so the filling of the surface with the first layer of molecules occurs in a narrow pressure range. The APD can be regarded as the negative derivative of the adsorption isotherm [3]. Note that the frequency curve of the distribution of APD is normalized to the volume of the monolayer of adsorbate.

The APD of various carbon black adsorbents was considered in [11], [12] in accordance with the degree of their crystallinity. The APD of highly graphitized samples of Carbopack F with high crystallinity showed three peaks at approximately 5.5, 3.0, and 0.7 kJ/mol. These signals were attributed to the formation of the nitrogen monolayer, to a two-dimensional fluid-solid transition and to the second layer formation, respectively. For the Carbopac X sample with the lowest degree of crystallinity, only the high-energy peak of the formation of the first monolayer at 5 kJ/mol was manifested. The authors [12] noted that the Carbopack samples with high SSA exhibited lower crystallinity, and they suggested that it might be difficult to obtain highly graphitized carbons with large SSA.

In our case, it may be noted that the closer the width and position of the APD peak for the GS samples to the peak for Carbopac F, the more perfect the structure of the adsorbing surface. For our GS samples in Fig. 3, only the first peak corresponding to the filling of the first monolayer is clearly manifested, the second peak corresponding to the phase transition is manifested as "noise" due to a small amount of matter in the sample (dashed curves in Fig. 3). For large samples of the TEG, the peaks at 5.5 and 3.0 kJ/mol are clearly visible. Note, in Fig. 3, the "ampoule effect" manifests itself in a faster rise in the frequency curve for GS samples that are smaller in weight and area.

One of the main parameters for adsorbents is the specific surface area (SSA). The definition of SSA BET [16] method is recommended and universally accepted [2], [17]. However, the choice of the isotherm points for the BET approximation in our case for a graphitized surface ($P/P_0 < 0.12$ [9]) is not sufficiently defined [8].

The possible range of the obtained SSA values is quite large, even within a high correlation coefficient. In the paper, the authors analysed the use of BET as an approximation for different isotherm sections with a correlation coefficient of at least 0.997 (Fig. 4).

From the physical point of view, for the application of the BET method, it is necessary to select an isotherm section for which adsorption proceeds only through a multilayer mechanism and processes of volume absorption in micropores or capillary condensation do not increase adsorption.

Another method for determining the SSA described by K.S.V. Sing is a comparative method of "alpha-s" [17].

40

The method consists in comparing the investigated isotherm with the reduced reference isotherm (alfa-s) for a nonporous sample. Reduction of the reference isotherm occurs by dividing the values of the isotherm by the value at pressure $P/P_0=0.4$. The investigated isotherm is compared with a reference isotherm for a related adsorbent for which a complete absence of pores is asserted and, hence, adsorption proceeds along a multilayer mechanism. At the same time, K.S.V. Sing indicated that in the case of similarity isotherms, SSA can be determined using a simple relation (1):

$$A_x/A_{ref} = S_x/S_{ref} \tag{1}$$

Moreover, the adsorption values A_x and A_{ref} were proposed to be used for the value of the relative pressure 0.4:

$$S_x = A_{x,0.4} \cdot S_{ref}/A_{ref,0.4} \tag{2}$$

In other words, if there are no other reasons, the difference in adsorption is due to the difference in specific areas.

The selection of another part of the isotherm for the determination of SSA was proposed and substantiated by K. Kaneko [15], [18] – the subtraction pore effect method (SPE).

The method is based on the fact that at low pressure, at which "alpha-s"<0.5, the pore filling swing occurs, and at higher pressure, when the "alpha-s">0.5 for graphitized materials an increase in adsorption occurs due to beginning of cooperative processes such as capillary condensation.

Therefore, the application of relation (1) occurs at the point "alpha-s"=0.5 or in a small rectilinear section near 0.5 (Fig. 5). For clarity, it is proposed to connect the origin with the isotherm point for "alfa-s"=0.5 and determine the SSA by the slope angle of the segment. The value "alpha-s"=0.5 corresponds to the relative pressure around $P/P_0=0.01$. To plot the curves in Fig. 5, the volume values on the required isotherm were recalculated to the pressure values on the reference isotherm by the method of linear interpolation.

Determination of the desired area with respect to the angle of the slope is the application of the same relation (2), only to the other point on the scale of pressure:

$$S_{x(Alfa=0,5)} = A_{x(Alfa=0,5)} \cdot S_{ref}/A_{ref(Alfa=0.5)} \tag{3}$$

To verify the performance of a multilayer process, one can construct the ratio $A_x \cdot S_{ref}/S_x \cdot A_{ref}$ as a function of pressure (Fig. 6). The multilayer process – P/P0 ranges from 0.1 to 0.4 – is clearly visible for the non-porous sample "KON" [18], in which the ratio is approximately equal to 1.

For GS samples, the ratio approaches unity within the range of 0.9–1.1 in the pressure region near $P/P_0=0.01$.

It is seen from Fig. 6 that the curves for GS, unlike the curves for a nonporous

sample and highly graphitized Carbopack F, raise sharply after a minimum at $P/P_0 \approx 0.1$.

This behaviour could be explained by the presence of a significant number of pores with a size of 2 nm and higher, but in our particular case, the rise is caused by adsorption on the walls of the ampoule.
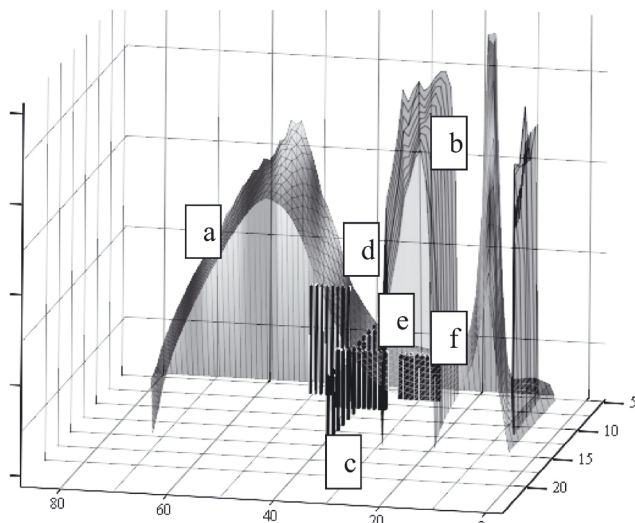

Fig. 4. BET surface calculated (a) for adsorption isotherms of the sample GS 1049. The horizontal axes represent: number start point (0 to 80) and the number of points (5 to 15) at which the SSA was calculated and located on the vertical axis. Surface (b) corresponds to a portion of the correlation coefficient that exceeds 0.997. Vertical segments (c, d, e, f,) are the bar plots which correspond to the places of SSA determination and height of the bars equal to the determined SSA. Segment (c) – points with pressure near 0.01 for SPE method; (d) – points for relative pressure 0.05–0.12; (e) – points with pressure near to 0.01 and correlation coefficient near 0.997; (f) – points for maximal correlation coefficient which corresponds to relative pressure of 0.0004–0.002.
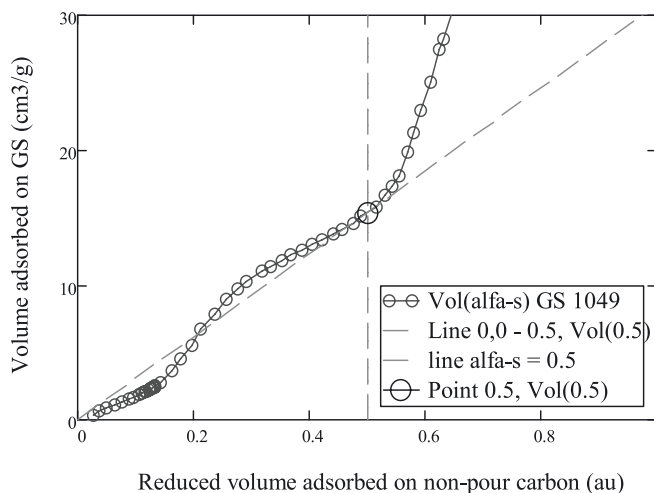

Fig. 5. Alfa–s plot. Volume adsorbed by GS sample (1049 Ni10mix069 1000rapidH2400) vs reduced volume adsorbed on reference non-porous carbon [19].
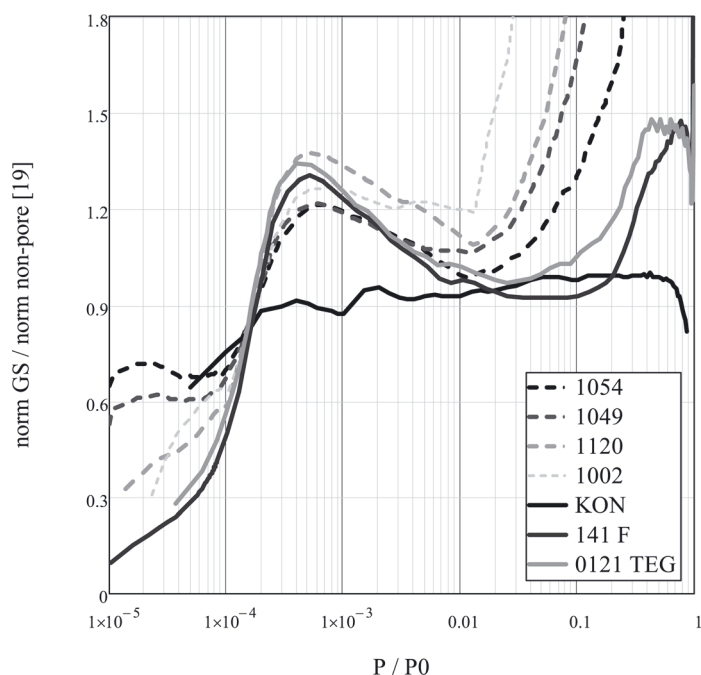
Fig. 6. Relationship $A_x \cdot S_{ref}/S_x \cdot A_{ref}$ between adsorption for some GS samples vs relative pressure. GS samples 1054, 1049, 1120; Sample 1141 F measured on highly graphitized Carbopack F (Aldrich); non-porous samples KON [18] and reference non-porous carbon [19].

Table 1 and Fig. 7 show the results of determination of SSA for a number of GS samples by BET methods in accordance with Fig. 4 and SPE in accordance with Fig. 5.

Table 1

The Results of Determination of SSA for GS Samples

SSA	GS №	1069	1040	1049	1110	1107	1054	1119	1002	1120
S BET, m²/g	0.0004 – 0.002	84.5	66.9	61	43.9	120.1	60.8	43.6	34	49.1
S BET, m²/g	P/P0=0.01	111.6	87.8	79.2	62.3	156.6	75.2	54	46.3	57.4
S SPE, m²/g	P/P0=0.01	116.8	93.8	84	70.3	157.5	74.7	56.2	47.4	63.1
S BET, m²/g	0.025–0.12	230.4	522.6	150.4	333.6	260.8	104	153.9	374.9	158.7
Thickness, Å	RTG "t"	85	104	83	107	38	88	116	91	111
GS weight from balance,g		0.0019	0.0012	0.0037	0.0015	0.0027	0.0052	0.0028	0.002	0.0034
Bulk density * of GS, mg/cm³		13.3	13.6	14.8	no	no	17.9	9.8	12.6	10
Area ** GS, m²	0.0004 – 0.002	0.16	0.08	0.22	0.06	0.32	0.31	0.12	0.07	0.17

* The density of GS samples was determined from the ratio of the weight in a dry state with respect to the wet weight (after boiling in water).

** The area of GS samples was determined from the multiplication of the weight of GS onto the SSA determined by the BET method in the range of $P/P_0 \sim 0.0004–0.002$
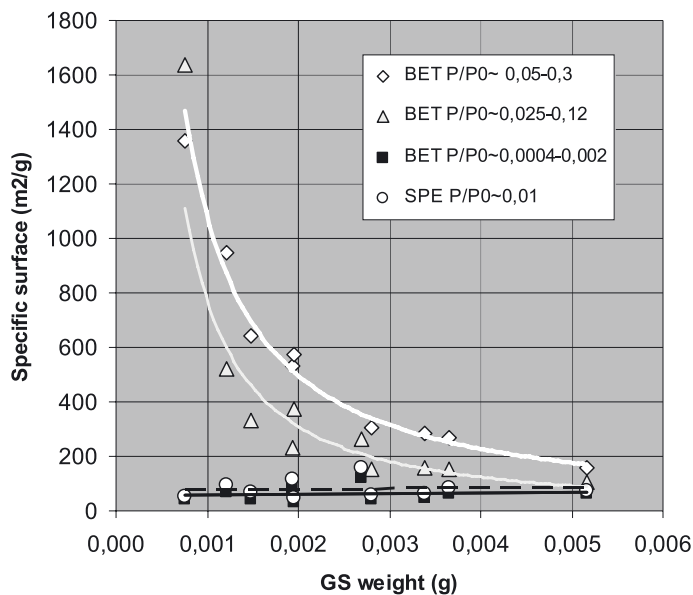
43

Fig. 7. SSA of GS samples determined with different ways by BET and SPE methodes and P/P0 regions. Lines - trendlines for SSA points. SSA determined at points of P/P0 0.0004 – 0.002 had a maximal correlation coefficient 0.9999. These points laid around of maximum at Fig. 8 or around knee at Fig. 2.
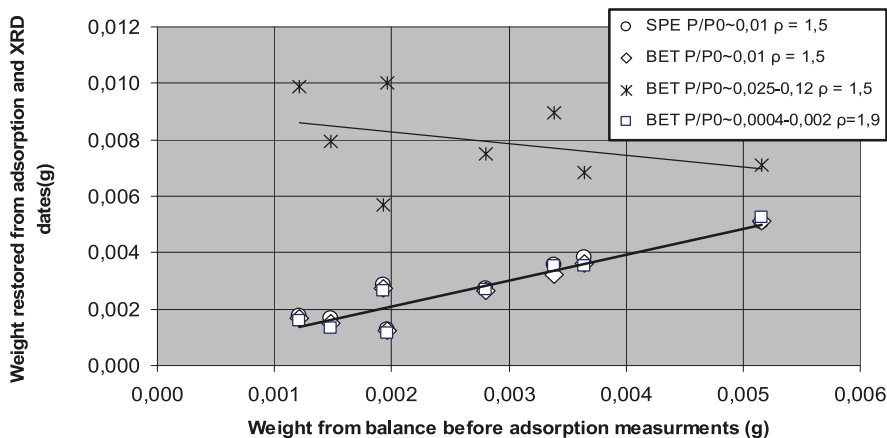

Fig. 8. Weight of GS samples restored from the data of N2 adsorption and XRD measurement. All symbols – weight restored from experimental data for different ways of SSA determination; BET and SPE; P/P0 regions and density ρ values. Lines – trendlines for calculated weight points.

It follows from Fig. 7 that the SSA values for different P/P_0 ranges have different dependencies on the weight of the GS samples. For low P/P_0 pressure less than or equal to 0.01, the SSA values are independent of weight, and for pressure greater than 0.01, the SSA values increase with a decrease in sample weight. The analysis shows that this is due to the fact that the adsorption value for such pressure is

determined not by the GS sample but also by the ampoule walls as indicated above (Fig. 2b).

The GS samples investigated in the first approximation can be represented as a set of multilayer graphene plates (Fig. 1c) with approximately the same thickness and density. The sample weight can be determined from adsorption data and XRD. Using SSA for each sample and its thickness (according to XRD), it is possible to calculate its weight by a simple ratio:

$$W = SSA \cdot w \cdot t \cdot \rho, \tag{5}$$

where w is the true (by weight) weight of the sample, t is the thickness, ρ is the density. At the same time, it becomes possible to compare different methods for determining SSA and to estimate the density of the objects – multilayer graphene plates based on the fact that the true weight is known. The results of the calculations are presented in Fig. 8. Figure 8 shows the weight points of the GS samples calculated from relation (5) for the SSA values obtained by the BET method from the pressure range of 0.025–0.12. A large scatter and complete lack of proportionality to the true weight indicate that these SSA values are erroneous and the isotherm path at this pressure range is associated with adsorption on the ampoule walls.

It follows from Fig. 8 that the weight values calculated for smaller P/P_0 values can be equated to the weight of the GS samples under the assumption that the density of multilayer graphene plates is either $\rho=1.5$ g/cm^3 for SSA in the P/P_0~0.01 region, or $\rho=1.9$ g/cm^3 for SSA values determined in the area of the maximum correlation of BET approximation for P/P_0~0.0004–0.002.

The value of the density of volumetric graphite is 2.3 g/cm^3 and the values from 1.5 to 1.9 g/cm^3 for a multilayer graphene plate are possible. Note that in this case it should be assumed that graphene plates have pores inaccessible to adsorption of nitrogen molecules.

On the other hand, based on the assumption that GS is a collection of multilayer graphene plates with approximately the same thickness, the formula for SSA is as follows:

$$SSA_{calc} = 1/(t \cdot \rho), \tag{6}$$

where t is the thickness, ρ is the density of the graphene plate. This formula is equivalent to formula (5) and is needed to check the correlation with another independent parameter – the thickness t obtained from the XRD data.

For each GS sample with specified thickness of the graphene layer, in Fig. 9 the SSA values were obtained by different methods (Fig. 4 and Fig. 5) and SSA calculated from the hyperbola formula (6) for two density values $\rho=1.5$ g/cc and $\rho=1.9$ g/cm^3 of a multilayer graphene plate. Figure 9 shows that the hyperbolas at such values of the density approximately correspond to the scatter of the experimental values of SSA.
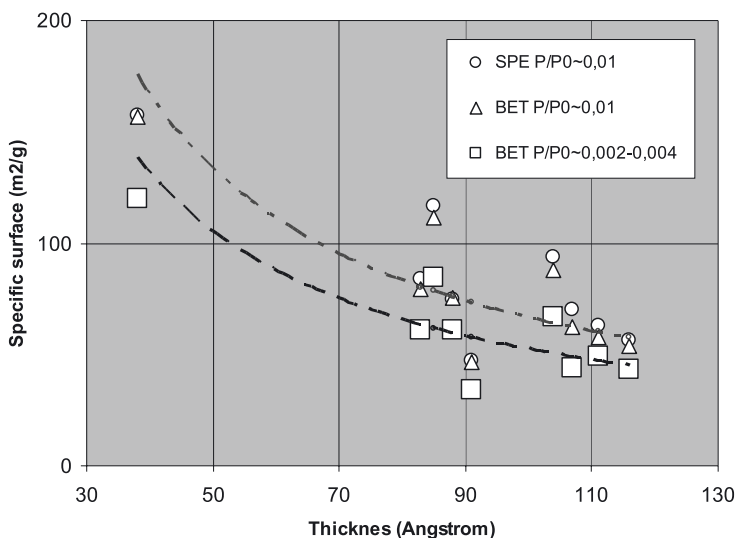
Fig. 9. SSA of GS samples vs thickness of multilayered graphene plates from XRD measurement. Circles, triangles, squares – experimental data for SSA determined in different ways; circles – by SPE metode; triangles – by BET method for P/P0 ~ 0.01; squares – by BET method for points at which BET approximations had a maximal correlation coefficient larger than 0.9999. These points had a range of P/P0 0.0002–0.004. Hyperbolic lines were calculated by formula (6) with density values ρ = 1.5 (upper) and ρ =1.9 g/cm^3 (lower).

Comparison of the initial section of adsorption isotherms for GS and well-graphitized objects – Carbopac F, graphite milled, TEG – has led to the conclusion that the surface of multilayer graphene plates in the GS is of good quality. The representation of our GS as a set of multilayer graphene plates (Fig. 1c) with approximately the same thickness and density made it possible to calculate the weight of the GS samples with a reasonable assumption of the graphene plate density ρ=1.9 g/cm^3. Note that the calculation did not take into account the adsorption at the edges of multilayer graphene plates, which was possible for large graphene sheets.

The longitudinal dimension of the La crystallite can be estimated from the width of the XRD peak (100), the obtained value La~10–12 nm [1]. The longitudinal size of the crystallites can also be estimated from the Raman scattering [20]; the values obtained are from one to several tens of nanometres. Note that the outer dimensions of multilayer graphene plates range from 0.1 to 1 μm. Under the assumptions outlined above, it is possible to evaluate the methods for determining SSA.

4. CONCLUSIONS

The research has demonstrated the difficulties of measuring the adsorption of nitrogen on ultralight GS samples with a mass of 1 to 5 mg and a bulk density of 10–15 mg/cm^3. The reason can be explained by the small area of the adsorbing surface of the samples of GS 0.1–0.3 m^2, which made it possible to obtain an adsorption isotherm for GS only for low relative pressure P/ P_0<0.01-0.015 due to the fact that within this pressure range adsorption on the walls of the ampoule does not practically occur (Fig. 2b). Note that the representation of adsorption data from small

objects shown in Fig. 2b is of methodological significance since it has allowed correctly estimating the size of the sample area relative to the effect of adsorption on the surface of the ampoule.

To obtain the SSA value corresponding to its geometric meaning, BET approximation in the range of 0.0004–0.002 P/P_0 should be used for our samples. This range corresponds to the best correlation coefficient of BET approximation and gives the lowest SSA values. From another point of view, this range corresponds to the primary filling of a well-crystallized graphite (or graphene) surface.

Further refinement of the true value of SSA requires additional experiments with GS samples with an adsorbing surface of 5–10 m^2 and independent estimates of the density of the graphene layer.

ACKNOWLEDGEMENTS

REFERENCES

1. Grehov, V., Kalnacs, J., Mishnev, A., & Kundzins, K. (2016). Synthesis of graphenic carbon materials on nickel particles with controlled quantity of carbon. *Latvian Journal of Physics and Technical Sciences, 53*, 56–12.

2. Schiith, F., Sing, K., & Weitkamp, J. (eds.) (2002). *Handbook of Porous Solids*. Weinheim: Wiley-VCH Verlag GmbH.

3. Bottani, E.J., & Tascon, J.M.D. (eds.) (2008). *Adsorption by Carbons*. Elsevier Ltd.

4. Inagaki, M., Qiu, J., & Guo, Q. (2015). Carbon foam: Preparation and application. *Carbon*, *87*,128–152.

5. Wu, R., Yu, B., Liu, X., Li, H., Wang, W., Chen, L., … Yang, S.T. (2016). One-pot hydrothermal preparation of graphene sponge for the removal of oils and organic solvents. *Appl. Surf. Sci., 362*, 56–63.

6. Novoselov, K.S., Geim, A.K., Morozov, S.V., Jiang, D., Zhang, Y, Dubonos, S.V., Firsov, A.A. (2004). Electric field effect in atomically thin carbon films. *Science*, *306*, 666–669.

7. Sun, H., Zhen Xu Z., & Gao, Ch. (2013). Multifunctional, ultra-flyweight, synergistically assembled carbon aerogels. *Advanced Materials, 25*, 2554-2560.

8. Grehov, V., Kalnacs, J., Matzui, L., Knite, M., Murashov, A., & Vilken, A. (2013). Nitrogen adsorption by thermoexfoliated graphite. *Latvian Journal of Physics and Technical Sciences*, *50*, 58-66.

9. Grehov, V., Kalnacs, J., Vilken, A., Mishnev, A., Knite, M., & Kundzins, K. (2015). Structural investigation of graphenic carbon materials obtained on nickel particles. *FM&NT-2015 Functional Materials and Nanotechnologies*, 115–115.

10. Tynan, M.K., Johnson, D.W., Dobson, B.P., & Coleman, K.S. (2016). Formation of 3D graphene foams on soft templated metal monoliths. *Nanoscale, 8*, 13303-13310.

11. Darmstadt, H., & Roy, C. (2001). Comparative investigation of defects on carbon black surfaces by nitrogen adsorption and SIMS. *Carbon, 39*, 841–849.

12. Kruk, M., Li, Z., Jaroniec, M., & Betz, W.R. (1999). Nitrogen adsorption study of sur-

face properties of graphitized carbon blacks. *Langmuir*, *15*, 1435–1441.

13. Sing, K.S.W., Everett, D.H., Haul, R.A.W., Moscou, L., Pierotti, A., Rouquerol, J., & Siemieniewska, T. (1985). Reporting physisorption data for gas/solid systems. *Pure & App Chem*, *57*(4), 603–619.

14. Ohba, T., Takase, A., Ohyama, Y., & Kanoh, H. (2013). Grand canonical Monte Carlo simulations of nitrogen adsorption on graphene materials with varying layer number. *Carbon, 61*, 40–47.

15. Setoyama, N., Suzuki, T., & Kaneko, K. (1998). Simulation study on the relationship between a high resolution a-s plot and pore size distribution for activated carbon. *Carbon, 36*, 1459–1467.

16. Brunauer, S., Emmett, P., & Teller, E. (1938). Adsorption of gases in multimolecular layers. *J. Amer. Chem. Soc., 60*, 309–319.

17. Грег, С., & Синг, К. (1984). Адсорбция, удельная поверхность, пористость. Москва: МИР.

18. Kaneko, K., Ishii, C., Ruike, M., & Kuwabara, H. (1992). Origin of superhigh surface area and microcrystalline graphitic structures of activated carbons. *Carbon*, *30*, 1075–1088.

19. Silvestre-Albero, A., Silvestre-Albero, J., Martı´nez-Escandell, M., Futamura, R., Itoh, T., Kaneko, K., & Rodrı´guez-Reinoso, F. (2014). Non-porous reference carbon for N2 (77.4 K) and Ar (87.3 K) adsorption. *Carbon*, *66*, 699–794.

20. Grehov, V., Kalnacs, J., Vilken, A., Mishnev, A., Chikvaidze, G., Knite, M., & Saharov, D. (2014). Graphene Nanosheets Grown on Ni Particles. *RCBJSF-2014-FM&NT*, 303-303.

SLĀPEKĻA ADSORBCIJA UZ GRAFĒNA SŪKĻIEM, TOS SINTEZĒJOT NIĶEĻA UN OGLEKĻA MAISĪJUMA IZKARSĒŠANAS UN ATLAIDINĀŠANAS REZULTĀTĀ.

V. Grehovs, J. Kalnačs, A. Mišņevs, K.Kundziņš

K o p s a v i l k u m s

Pētīta grafēna sūkļu sorbcijas spēja, to raksturojot ar īpatnējo absorbcijas virsmas laukumu. Nosakot īpatnējā virsmas laukuma lielumu izmantota Brunauera, Emmeta, Tellera (BET) metode izotermu aproksimācijai spiedienu diapazonā 0.025-0.12. Parādīts, ka BET metode šajā diapazonā uzrāda lielas kļūdas, jo gadījumos, kad īpatnējais laukums relatīvi mazs 0,1 līdz 0,3 m^2 netiek ņemta vērā adsorbcija uz ampulas sienām, kura ir salīdzināma vai lielāka nekā absorbcija uz pētāmā objekta.

Reāli dati par grafēna sūkļu īpatnējo absorbcijas virsmu iegūstami ar poru efekta atskaitīšanas metodi (angļu – subtracting por effect - SPE method), vai tad, ja BET aproksimāciju izmanto mazu relatīvo spiedienu P/P_0 diapazonā 0,0004 – 0,002.

21.05.2017.